Resonance states and quantum tunneling of Bose-Einstein condensates in a three-dimensional shallow trap

Sudip Kumar Haldar,[1] Barnali Chakrabarti,[1] and Tapan Kumar Das[2]
[1]*Department of Physics, Lady Brabourne College, P-1/2 Suhrawardy Avenue, Calcutta 700017, India*
[2]*Department of Physics, University of Calcutta, 92 A.P.C. Road, Calcutta 700009, India*
(Received 7 May 2010; published 20 October 2010)

A correlated quantum many-body method is applied to describe resonance states of atomic Bose-Einstein condensates (BEC) in a realistic shallow trap (as opposed to the infinite traps commonly used). The realistic van der Waals interaction is adopted as the interatomic interaction. We calculate experimentally measurable decay rates of the lowest quasibound state in the shallow trap. The most striking result is the observation of a metastable branch besides the usual one for attractive BEC in a pure harmonic trap. As the particle number increases the metastable branch appears and then gradually disappears, and finally the usual metastable branch (associated with the attractive BEC in a harmonic trap) appears, eventually leading to the collapse of the condensate.

DOI: 10.1103/PhysRevA.82.043616 PACS number(s): 03.75.Hh, 31.15.xj, 03.65.Ge, 03.75.Nt

I. INTRODUCTION

In experiments with Bose-Einstein condensation (BEC), the evolution of the atomic cloud and its instability strongly depends on the external confinement, which is usually chosen as either isotropic or anisotropic pure (i.e., of infinite extent) harmonic potential. But, in the actual experimental setup, the trap is of finite extent. During the last few years, attention has been shifted to shallow optical dipole traps [1]. As the quadratic trapping potential takes the shallow Gaussian envelope form, the anharmonicity of the potential must be taken into account. BEC in such a shallow trap of finite width supports resonance states which are quasibound. In such an experimental trap, the decay mechanism of the condensate becomes an important issue, as the condensate can escape from the trapping potential by quantum tunneling through intermediate barriers, in addition to the usual collapse of attractive condensates. Several attempts have been made to calculate the lifetimes of quasibound states and to study the transition from a resonance to a bound state by solving the Gross-Pitaevskii equation (GPE) using contact δ interaction [2–6]. The GPE is based on the mean-field description and ignores correlations in the many-body wave function. But near the criticality, the energy of the resonance state becomes very close to the barrier height and the condensate becomes highly correlated. Thus incorporation of interatomic correlation becomes important. Naturally the full quantum many-body treatment incorporating a realistic interatomic interaction is indeed necessary. In particular the present experiments consider only a finite number of atoms in the external trap. Such condensates are quantum depleted, which again deserve a full quantum many-body treatment. The external shallow potential can be modeled by a quadratic plus a quartic potential, viz., $V(r) = \frac{1}{2}m\omega^2 r^2 + \lambda r^4$, where λ is the anharmonic parameter. In our earlier work in this direction, we investigated the ground-state properties in such a trap. We also observed dramatic change in the stability factor $\frac{N_{\rm cr}|a_{\rm sc}|}{a_{\rm ho}}$ (where $N_{\rm cr}$ is the critical number of atoms beyond which the attractive condensate collapses) due to the anharmonicity [7].

Thus the aim of our present work is to employ a correlated quantum many-body approach incorporating a finite-range realistic interatomic interaction to study resonance states in shallow traps. We calculate decay rates of quasibound condensates and study how the interatomic interaction and the anharmonicity interfere with the decay process. Deviations from earlier works which used the mean-field equation can be attributed to two-body correlations and a finite range of the realistic interaction. Due to the realistic nature of our calculation we expect results which are relevant to experiments. We observe resonance states associated with an unusual metastability for the repulsive BEC. The most striking result is the observation of two metastable branches for an attractive BEC. The attractive BEC containing N atoms in a pure harmonic trap is associated with a metastable branch, which ultimately collapses for $N > N_{\rm cr}$. In the present study we observe that, with an increase in particle number, a metastability first appears and then gradually disappears, and finally the usual metastability (associated with attractive BEC in a pure harmonic trap) appears, eventually leading to the collapse. We also study macroscopic quantum tunneling and calculate decay rates for these two branches.

In Sec. II we introduce the methodology which contains the many-body approach used in this work based on the correlated potential harmonic expansion method. Section III contains numerical results and discussions. Conclusions are drawn following a summary of our work in Sec. IV.

II. CORRELATED POTENTIAL HARMONIC EXPANSION METHOD (CPHEM)

We adopt the potential harmonic expansion method with a short-range correlation function which has already been established as a very successful and useful technique for the study of dilute BEC [8–10]. Here we describe the technique briefly.

We consider that a system of $A = (N + 1)$ identical bosons, each of mass m, is confined in an external trap $[V_{\rm trap}(r)]$ which is modeled as a harmonic potential (of frequency ω) perturbed by a quartic term. The time-independent quantum many-body

Schrödinger equation is written as

$$\left[-\frac{\hbar^2}{2m}\sum_{i=1}^{A}\nabla_i^2 + \sum_{i=1}^{A} V_{\rm trap}(\vec{x}_i) + \sum_{i,j>i}^{A} V(\vec{x}_i - \vec{x}_j) - E \right] \times \Psi(\vec{x}_1,\ldots,\vec{x}_A) = 0, \quad (1)$$

where E is the total energy of the system, $V(\vec{x}_i - \vec{x}_j)$ is the two-body potential, and $\vec{x}_i$ is the position vector of the ith particle. We define a set of N Jacobi vectors as

$$\vec{\zeta}_i = \sqrt{\frac{2i}{i+1}}\left(\vec{x}_{i+1} - \frac{1}{i}\sum_{j=1}^{i}\vec{x}_j\right)(i = 1,\ldots,N). \quad (2)$$

The center of mass coordinate is $\vec{R} = \frac{1}{A}\sum_{i=1}^{A}\vec{x}_i$. As the labeling of particles is arbitrary, we choose the relative separation of the (ij)-interacting pair $(\vec{x}_{ij} = \vec{x}_i - \vec{x}_j)$ as $\vec{\zeta}_N$. We define the hyperradius r as [11]

$$r^2 = \sum_{i=1}^{N}\zeta_i^2 = \frac{2}{A}\sum_{i,j>i}^{A} x_{ij}^2 = 2\sum_{i=1}^{A} r_i^2, \quad (3)$$

where $\vec{r}_i = \vec{x}_i - \vec{R}$ is the position vector of the ith particle with respect to the center of mass of the system. The relative motion of the bosons is given by

$$\left[-\frac{\hbar^2}{m}\sum_{i=1}^{N}\nabla_{\zeta_i}^2 + V_{\rm trap} + V_{\rm int}(\vec{\zeta}_1,\ldots,\vec{\zeta}_N) - E_R \right] \times \Psi(\vec{\zeta}_1,\ldots,\vec{\zeta}_N) = 0, \quad (4)$$

where $V_{\rm trap}$ is the effective external trapping potential and $V_{\rm int}$ is the sum of all pairwise interactions. E_R is the relative energy of the system, that is, $E = E_R + \frac{3}{2}\hbar\omega$. The laboratory BEC is designed to be very dilute, so that the probability of three or more atoms coming within the range of interaction is negligible. This is done in laboratory experiments, in order to avoid molecule formation through three-body collisions. Hence, when the (ij) pair interacts, the rest of the atoms are far apart and are inert spectators. Therefore, only two-body correlations in the many-body wave function and pairwise interactions among atoms are important. For the (ij)-interacting pair, we define a hyperradius ρ_{ij} for the remaining $(N-1)$ noninteracting bosons as [12]

$$\rho_{ij} = \sqrt{\sum_{K=1}^{N-1}\zeta_K^2}, \quad (5)$$

so that $r^2 = x_{ij}^2 + \rho_{ij}^2$. A hyperangle ϕ is introduced through $x_{ij} = r\cos\phi$ and $\rho_{ij} = r\sin\phi$. The full set of $3N$ hyperspherical variables is chosen as

(a) r,ϕ,ϑ,φ (ϑ and φ are the polar angles of $\vec{x}_{ij}$ corresponding to the interacting pair), and

(b) $(3N-4)$ hyperangular variables associated with the remaining $(N-1)$ inert spectators. Out of these, $2(N-1)$ are the polar angles associated with $(N-1)$ Jacobi vectors and another $(N-2)$ "hyperangles" define their relative lengths.

In the potential harmonic expansion method (PHEM), we decompose the many-body wave function(Ψ) into Faddeev components ϕ_{ij} for the (ij)-interacting pair as

$$\Psi = \sum_{i,j>i}^{A}\phi_{ij}(\vec{x}_{ij},r)\cdot \quad (6)$$

Then Eq. (4) can be expressed as

$$[T + V_{\rm trap} - E_R]\phi_{ij} = -V(\vec{x}_{ij})\sum_{kl>k}^{A}\phi_{kl} \quad (7)$$

where

$$T = -\frac{\hbar^2}{m}\sum_{i=1}^{N}\nabla_{\zeta_i}^2.$$

Since only two-body correlations are relevant, the Faddeev component ϕ_{ij} is independent of the coordinates of all the particles other than the interacting pair. Hence the total hyperangular momentum quantum number as also the orbital angular momentum of the whole system (composed of all bosons) is contributed by the interacting pair only. We expand ϕ_{ij} in the subset of hyperspherical harmonics (HH) necessary for the expansion of $V(\vec{x}_{ij})$. Thus

$$\phi_{ij}(\vec{x}_{ij},r) = r^{-\left(\frac{3N-1}{2}\right)}\sum_{K}\mathcal{P}_{2K+l}^{lm}\left(\Omega_N^{ij}\right)u_K^l(r), \quad (8)$$

where Ω_N^{ij} denotes the full set of hyperangles in the $3N$-dimensional space corresponding to the (ij)-interacting pair. This new basis set $\{\mathcal{P}_{2K+l}^{lm}(\Omega_N^{ij})\}$ is called the potential harmonics (PH) basis and it is independent of $(\vec{\zeta}_1,\ldots,\vec{\zeta}_{N-1})$. Thus the total angular momentum of the condensate and its projection are simply l and m, which comes from the interacting pair, and all other quantum numbers coming from $(N-1)$ noninteracting bosons are kept frozen. An analytic form of the potential harmonics can be found in Ref. [12]. Substitution of Eq. (8) into Eq. (7) and taking projection on a particular PH gives [8]

$$\left[-\frac{\hbar^2}{m}\frac{d^2}{dr^2} + \frac{\hbar^2}{m}\frac{\mathcal{L}_K(\mathcal{L}_K+1)}{r^2} + V_{\rm trap}(r) - E_R \right]U_K^l(r), + \sum_{K'} f_{K'l}^2 V_{KK'}(r)U_{K'}^l(r) = 0, \quad (9)$$

where $V_{KK'}$ is the potential matrix and is given by

$$V_{KK'}(r) = \int P_{2K+l}^{lm^*}\left(\Omega_N^{ij}\right)V(x_{ij})P_{2K'+1}^{lm}\left(\Omega_N^{ij}\right)d\Omega_N^{ij}, \quad (10)$$

where $\mathcal{L}_K = 2K + l + \frac{3N-3}{2}$ and f_{Kl}^2 is the overlap of the PH for ij partition with the sum of PHs of all partitions [8]. K is the grand orbital quantum number in $3N$-dimensional space. All other intermediate angular momentum quantum numbers take zero eigenvalues. As the number of active variables is now *only four* (global hyperradius r and three others for $\vec{x}_{ij}$) for any number of bosons, the numerical complication is greatly

simplified. Equation (9) can be put in symmetric form as

$$\left\{ -\frac{\hbar^2}{m}\frac{d^2}{dr^2} + V_{\rm trap}(r) + \frac{\hbar^2}{mr^2}[\mathcal{L}(\mathcal{L}+1) + 4K(K+\alpha+\beta+1)] - E_R \right\} U_{Kl}(r) + \sum_{K'} f_{Kl} V_{KK'}(r) f_{K'l} U_{K'l}(r) = 0, \quad (11)$$

where $\mathcal{L} = l + \frac{3A-6}{2}$, $U_{Kl} = f_{Kl} u^l_K(r)$, $\alpha = \frac{3A-8}{2}$ and $\beta = l + 1/2$.

In experimentally achieved BEC, because the energy of the interacting pair is extremely small, the two-body interaction is reproduced by the s-wave scattering length ($a_{\rm sc}$). Positive (negative) $a_{\rm sc}$ corresponds to a repulsive (attractive) condensate. In the Gross-Pitaevskii equation, the interatomic interaction is a contact interaction and is absolutely determined by its strength $a_{\rm sc}$ only. Thus the two-body potential is purely repulsive or purely attractive, depending on the sign of $a_{\rm sc}$. But the van der Waals potential has two terms, one part represents a strong repulsion (usually represented by a hard core of radius r_c) at very short separation and the other part goes by $-\frac{C_6}{x_{ij}^6}$, and $a_{\rm sc}$ can be either positive or negative depending on the value of r_c [9]. Thus we determine $a_{\rm sc}$ by solving the zero-energy two-body Schrödinger equation for the two-body wave function $\eta(x_{ij})$:

$$-\frac{\hbar^2}{m}\frac{1}{x_{ij}^2}\frac{d}{dx_{ij}}\left(x_{ij}^2\frac{d\eta(x_{ij})}{dx_{ij}}\right) + V(x_{ij})\eta(x_{ij}) = 0. \quad (12)$$

The value of $a_{\rm sc}$ is determined from the asymptotic part of $\eta(x_{ij})$ [13]. The zero-energy two-body wave function $\eta(x_{ij})$ is also a good representation of the short-range behavior of ϕ_{ij} and is taken as the two-body correlation function in the PH expansion basis to improve the rate of convergence [14]. Thus in the CPHEM, we replace Eq. (8) by

$$\phi_{ij}(\vec{x}_{ij}, r) = r^{-(\frac{3N-1}{2})} \sum_K \mathcal{P}^{lm}_{2K+l}(\Omega^{ij}_N) u^l_K(r)\eta(x_{ij}). \quad (13)$$

Introduction of $\eta(x_{ij})$ enhances the rate of convergence of the PH expansion dramatically. This has been actually verified in our numerical calculation. In our numerical procedure we solve Eq. (12) for the zero-energy two-body wave function $\eta(x_{ij})$ in the chosen two-body potential $V(x_{ij})$. We adjust the hard-core radius r_c, such that a_{sc} has the desired value [9,13]. This $\eta(x_{ij})$ is then used in Eq. (13) and the potential matrix becomes

$$V_{KK'}(r) = \left(h^{\alpha\beta}_K h^{\alpha\beta}_{K'}\right)^{-\frac{1}{2}} \int_{-1}^{+1} \left[P^{\alpha\beta}_K(z) V\left(r\sqrt{\frac{1+z}{2}}\right) \times P^{\alpha\beta}_{K'}(z)\eta\left(r\sqrt{\frac{1+z}{2}}\right) W_l(z)\right] dz, \quad (14)$$

where $P^{\alpha\beta}_K(z)$ is the Jacobi polynomial, and its norm and weight function are $h^{\alpha\beta}_K$ and $W_l(z)$, respectively [15]. We truncate the K sum in Eq. (13) to an upper limit $K_{\rm max}$, providing the desired convergence. Finally the coupled differential equation (CDE), Eq. (11), is solved by the hyperspherical adiabatic approximation (HAA) [16]. In the HAA, one assumes that the hyperradial motion is slow compared to the hyperangular motion. Hence the latter is separated adiabatically and solved for a particular value of r, by diagonalizing the potential matrix together with the diagonal hypercentrifugal repulsion in Eq. (11). The lowest eigenvalue, $\omega_0(r)$ [corresponding eigencolumn vector being $\chi_{K0}(r)$], provides the effective potential for the hyperradial motion. We choose the lowest eigenpotential [$\omega_0(r)$] as the effective potential in which the entire condensate moves as a single entity. Thus in the HAA, the approximate solution (the energy and wave function) of the condensate is obtained by solving a single uncoupled differential equation,

$$\left[-\frac{\hbar^2}{m}\frac{d^2}{dr^2} + \omega_0(r) - E_R \right] \zeta_0(r) = 0, \quad (15)$$

subject to appropriate boundary conditions on $\zeta_0(r)$. The function $\zeta_0(r)$ is the collective wave function of the condensate in the hyperradial space. The lowest-lying state in the effective potential $\omega_0(r)$ corresponds to the ground state of the condensate. The total energy of the condensate is obtained by adding the energy of the center of mass motion ($\frac{3}{2}\hbar\omega$) to E_R.

The main advantages of our CPHEM are the following.

(i) Potential harmonic basis keeps all possible two-body correlations and yet the number of variables is reduced to only *four* for any number of bosons in the trap. So despite incorporating all the two-body correlations, we can treat quite a large number of atoms in the trap without much numerical complication.

(ii) We can use a realistic interatomic interaction like the van der Waals potential having a finite range, which itself takes care of the short-range repulsion and interatomic correlations.

(iii) Unlike the GPE, CPHEM does not have any pathological singularity, since the two-body interaction is a realistic one and has a strong short-range repulsion.

Thus the CPHEM reveals the realistic picture. Clearly it is an improvement over the GPE. Finally, by using the HAA, we reduce the multidimensional problem into an effective one-dimensional one in hyperradial space and the effective potential $\omega_0(r)$ of this one-dimensional problem provides a clear qualitative picture and a quantitative description of the system.

III. RESULTS

We choose the interatomic potential as the van der Waals potential with a hard core of radius r_c, viz., $V(x_{ij}) = \infty$ for $x_{ij} \leqslant r_c$ and $= -\frac{C_6}{x_{ij}^6}$ for $x_{ij} > r_c$. The strong short-range repulsion is parametrized by the hard core and the strength (C_6) is known for a given type of atom, for example, $C_6 = 6.4898 \times 10^{-11}$ o.u. for Rb atoms [13]. The value of r_c is adjusted to get the desired value of $a_{\rm sc}$. In oscillator unit (o.u.), length and energy are given in the units of $a_{\rm ho} = \sqrt{\frac{\hbar}{m\omega}}$ and $\hbar\omega$, respectively. As $C_6 \to 0$, the potential becomes a hard-core potential and r_c coincides with the s-wave scattering length. As detailed in the previous section, we solve the zero-energy two-body Schrödinger equation for the interacting pair to get the value of r_c, which corresponds to the experimental scattering length $a_{\rm sc}$. With a tiny change in r_c, $a_{\rm sc}$ may change by a large amount, including sign [13]. With each additional

change in sign, the potential supports an extra two-body bound state resulting in an additional node in $\eta(x_{ij})$. Thus the choice of r_c is very crucial. We choose r_c such that it corresponds to the zero node in the two-body wave function for attractive interaction and one node for repulsive interaction [10]. For a repulsive BEC we choose ^{87}Rb atoms with $a_{sc} = 0.004\,33$ o.u. as in the JILA trap [17]. For an attractive BEC, we choose $a_{sc} = -1.832 \times 10^{-4}$ o.u., which is one of the values as reported in the controlled collapse experiment of ^{85}Rb atoms [18,19]. In both cases r_c is determined by the method discussed above.

In the optical dipole trap, the trapping potential takes the shallow Gaussian form and the external trap is given by $V(r) = \frac{1}{2}r^2 + \lambda r^4$. For $\lambda > 0$ the frequency is blue shifted and for $\lambda < 0$ the frequency is red shifted. In the experiment [20,21], quartic confinement is created with a blue detuned Gaussian laser directed along the axial direction. The nonrotating condensate was cigar shaped and the strength of the quartic confinement was $\approx 10^{-3}$. In the present study we choose λ as a controllable parameter and $|\lambda| \ll 1$. For $\lambda > 0$, as the quartic confinement becomes more tight, the frequency will increase for repulsive BEC and the attractive BEC will again be associated with a metastability [7]. These have been studied earlier in both one and three dimensions [22,23]. However, the most dramatic features are expected for $\lambda < 0$, and the potential can be easily approximated as $V(r) = \frac{1}{2}r^2 \exp(-cr^2)$ with $\lambda \approx \frac{c}{2}$. Our present calculation considers only $\lambda < 0$.

A. Repulsive BEC

For harmonic trapping with repulsive interaction, the condensate is always stable for any number of bosons. However, due to the presence of anharmonicity we observe a new and different metastablity of the condensate. In Fig. 1 we plot the effective potential $\omega_0(r)$ as a function of r for 500 atoms of ^{87}Rb in a shallow trap corresponding to $\lambda = -2 \times 10^{-5}$ o.u. and $a_{sc} = 0.004\,33$ o.u. We observe a dramatic change in the effective potential from that of a purely harmonic trap: a metastable region (MSR) appears bounded by an intermediate barrier on the right side (RIB), beyond which $\omega_0(r)$ decreases gradually, where the quartic term dominates over the quadratic term. In our earlier work [7], we studied how the ground-state properties and the low-energy collective excitations get modified due to anharmonicity and calculated the stability factor $\frac{N_{cr}|a_{sc}|}{a_{ho}}$ in such a shallow trap. In the present work, we calculate the decay rate of quasibound states in the MSR, as the metastable condensate will tunnel through the intermediate barrier. The macroscopic tunneling rate is calculated semiclassically by the WKB tunneling formula:

$$\Gamma_N^{\text{tunnel}} = N\nu \exp\left(-2\int_{r_1}^{r_2} \sqrt{2[\omega_0(r) - E]}\, dr\right) = N\nu \exp(-2\sigma), \tag{16}$$

where the limits of integration r_1 and r_2 are the inner and outer turning points of the intermediate barrier on the right (RIB) of $\omega_0(r)$, E is the energy of the metastable condensate, and $\exp(-2\sigma)$ is the WKB tunneling probability. The frequency of impact (ν) of the condensate on the RIB is approximately given by

$$\nu \sim \left(2\int_{r_0}^{r_1} \frac{dr}{\sqrt{2\,[E - \omega_0(r)]}}\right)^{-1}, \tag{17}$$

where r_0 and r_1 are the classical turning points of the metastable region. As N increases, the net effect of the negative anharmonicity increases fairly rapidly. Hence, even though the minimum and stiffness of $\omega_0(r)$ increases with N, the difference ($\Delta\omega$) of the maximum of RIB ($\omega_{\max}$) and the minumum of the MSR ($\omega_{\min}$) decreases with increasing N. Consequently, RIB disappears ($\Delta\omega = 0$) when N exceeds a critical value, N_{cr}^{first} [to distinguish the critical numbers associated with the right side and the left side (see later in this article) barriers, we name them as N_{cr}^{first} and N_{cr}^{second}, respectively]. This causes a new type of instability and eventual collapse. The tunneling rate is appreciable only when E is close to $\omega_{\max}$, and it increases rapidly as E approaches $\omega_{\max}$. In Fig. 2, the tunneling rate (Γ_N^{tunnel}) of the lowest resonance state is plotted against the number of condensate atoms close to

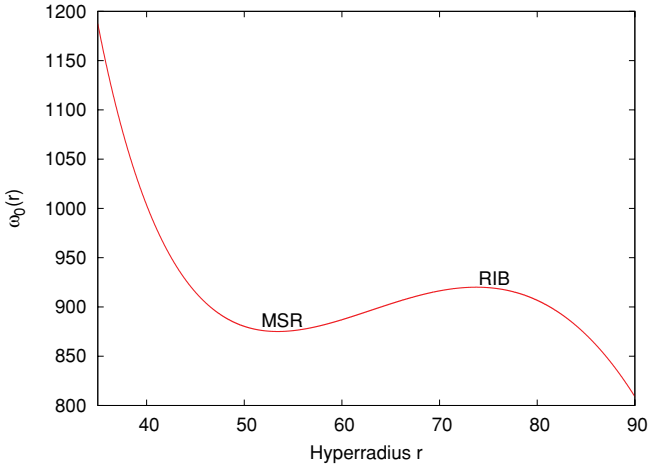

FIG. 1. (Color online) Plot of the effective potential $\omega_0(r)$ against r (both expressed in appropriate o.u.) for $N = 500$ atoms of ^{87}Rb with $a_{sc} = 0.004\,33$ o.u. and $\lambda = -2 \times 10^{-5}$ o.u. The metastable region (MSR) and the intermediate barrier on the right side (RIB) are indicated in the figure.

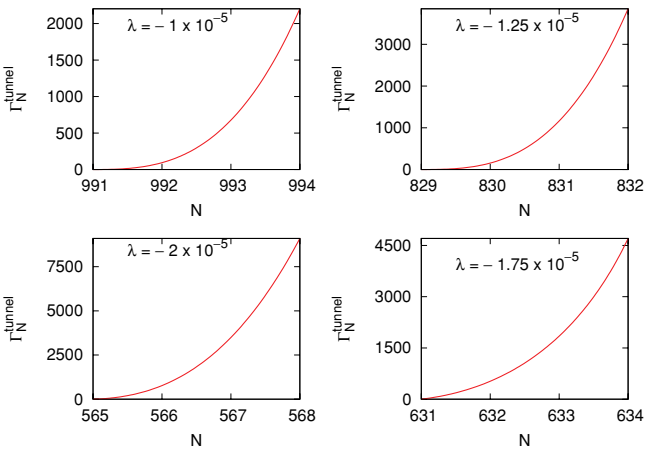

FIG. 2. (Color online) Plot of Γ_N^{tunnel} (in atoms per second) vs N for the lowest resonance state near the criticality for various values of λ (in o.u.).

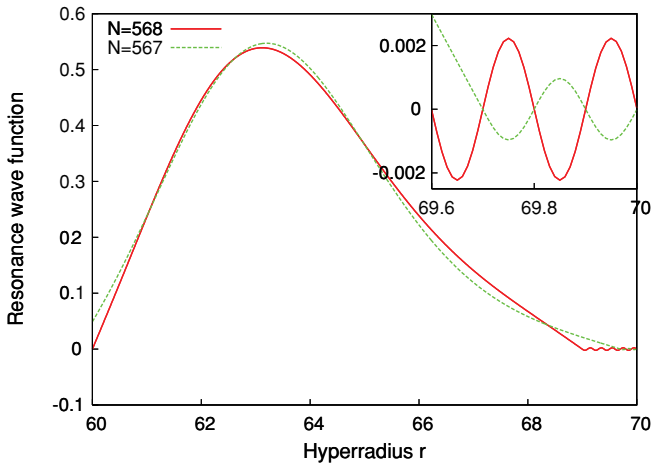

FIG. 3. (Color online) Plot of the resonance wave function (in o.u.) vs r (in o.u.) for $N = 567$ and $N = 568$ for $\lambda = -2 \times 10^{-5}$ o.u. and $a_{sc} = 0.004\,33$ o.u.. The oscillatory part of the wave function immediately outside the barrier is shown magnified in the inset.

the critical point for various values of anharmonic distortion. Near the criticality $N \sim N_{cr}^{first}$, the macroscopic tunneling is quite high and observation of this tunneling may be possible experimentally. The sharp peak near the criticality is attributed to the fact that the energy of the resonance state is close to the barrier height. Note that with increasing anharmonicity the right-side barrier becomes lower, which makes Γ_N^{tunnel} larger. For example, for $\lambda = -1.75 \times 10^{-5}$ o.u., the lowest resonance state near the critical point has a tunneling probability of 30%, whereas for $\lambda = -2 \times 10^{-5}$ o.u. the corresponding tunneling probability increases to 74%. Consequently, N_{cr}^{first} decreases with increasing $|\lambda|$.

In Fig. 3, we plot the resonance wave functions for two values of N close to critical point (viz., $N = 567$ and $N = 568$, the critical number being $N_{cr}^{first} = 570$). The wave function within the metastable region is large and it has a small oscillatory part just outside the RIB. This clearly signifies that a part of the wave function leaks. For better clarity, the rapidly oscillatory part of the wave function is shown magnified in the inset of Fig. 3. Note that the amplitude of the leaked part increases as N increases. At the critical point ($\Delta\omega = 0$) the metastable region disappears and the whole wave function leaks, which corresponds to the collapse. The picture is qualitatively the same as that observed for attractive BEC in a pure harmonic trap. However the phenomena near the present collapse is a bit different from the commonly observed collapse of attractive BEC in a harmonic trap. In the latter case the metastable region is associated with a deep attractive well on the left side of the MSR, the metastable condensate tunnels through the left intermediate barrier (LIB) near the origin and settles down in the deep well to form clusters. In a typical attractive condensate we have checked that the size of the well is $\sim$0.05 μm. Hence, due to the high two-body and three-body collision rates within such a narrow well, atoms form clusters. The width of this wave function in the narrow well is of the order of 0.003 μm, which is the order of the size of the atomic cluster. But in the present case the atoms which escape by tunneling outward will form a noncondensed Bose gas.

TABLE I. Decay rates of lowest resonance states for different λ in a repulsive BEC ($a_{sc} = 0.004\,33$ o.u.).

$\lambda = -1 \times 10^{-5}$ o.u.		$\lambda = -2 \times 10^{-5}$ o.u.	
$\lvert Na_{sc}\rvert$ (o.u.)	Γ_N^{tunnel} (atoms/s)	$\lvert Na_{sc}\rvert$ (o.u.)	Γ_N^{tunnel} (atoms/s)
4.304 02	2202.6475	2.459 44	9096.678 62
4.299 69	53.7088	2.455 11	1738.7188
4.295 36	1.3083	2.450 78	108.5416
4.291 03	0.1107	2.446 45	1.5149
4.286 70	0.0158	2.442 12	0.1794

As a further study to observe transition from a resonance state to a bound state, we calculate decay rates for different values of effective interaction $|Na_{sc}|$. By decreasing the effective repulsive interaction, we effectively enhance attraction between the atoms. Table I clearly shows that even for a very slow decrease in $|Na_{sc}|$, Γ_N^{tunnel} decreases rapidly and very soon reaches a vanishingly small value, which manifests the transition from resonance to a bound state.

Our result is qualitatively similar to earlier findings of Moiseyev *et al.* [2] where the transition from resonance to bound state was discussed. However the earlier calculations [2,5] used singular δ-function potential in the mean-field equation, and a negative offset potential was required to facilitate conversion of a quasibound state into a bound state, in a three-dimensional BEC. In our present calculation we need no such offset. This deviation from GPE results is attributed to the use of a realistic interatomic interaction having a hard-core repulsive part at shorter separation. Moreover, our results provide realistic aspects which are relevant to experiments.

B. Attractive BEC

The situation becomes more interesting for the attractive BEC in a shallow trap. We choose a condensate of ^{85}Rb atoms with $a_{sc} = -1.832 \times 10^{-4}$ o.u. For a clear understanding, we plot the effective potential in Fig. 4. The intermediate MSR is now bounded by two neighboring barriers, one on the left (LIB) and one on the right (RIB) of unequal height. On the left side of LIB, a deep and narrow attractive well (NAW) appears. In the same vertical scale, we could not plot this deep well; hence it is not shown in Fig. 4. The RIB is the effect of negative anharmonicity, which basically corresponds to a finite optical trap, whereas the LIB is the effect of the negative a_{sc}, which is commonly seen for attractive BEC in pure harmonic trap. The heights of the two barriers very strongly depend on two factors: first the anharmonic parameter and second the effective attractive interaction. Basically there is a competition between these two effects which causes the shape of the effective potential to change in a complicated fashion with the increase in N. So throughout our study we fix $\lambda = -9.37 \times 10^{-6}$ o.u. and the effective attractive interaction is tuned by changing the number of bosons. The metastable condensate will have a

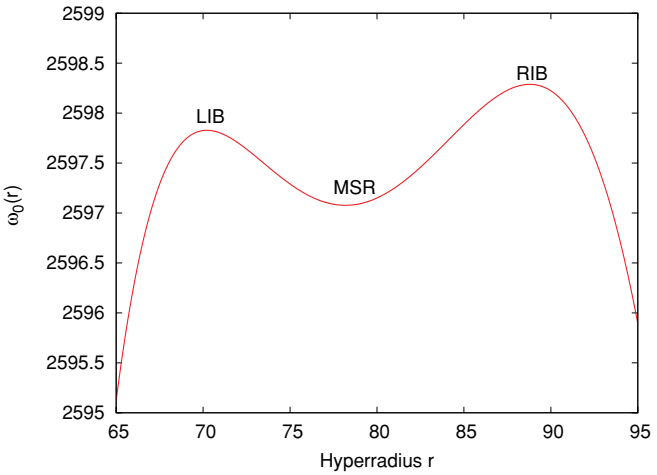

FIG. 4. (Color online) Plot of the effective potential $\omega_0(r)$ in o.u. against hyperradius r in o.u. for a condensate of ^{85}Rb atoms with $N = 2660$, $\lambda = -9.37 \times 10^{-6}$ o.u., and $a_{sc} = -1.832 \times 10^{-4}$ o.u..

finite probability of macroscopic quantum tunneling through both the barriers.

We start with few hundreds ^{85}Rb atoms in the trap, the two neighboring barriers are quite high and tunneling of the condensate through either of them is negligible. We have checked that in such a situation there is no substantial leakage of the condensate through the associated barriers. With further increase in particle number, we observe that the metastable region gradually becomes flatter, the corresponding condensate wave function expands slowly. With this wave function we calculate the average size of the condensate (r_{av}) [24] as the root-mean-square distance of individual atoms from the center of mass of the condensate:

$$r_{av} = \left\langle \frac{1}{A}\sum_{i=1}^{A}(\vec{x}_i - \vec{R})^2 \right\rangle^{1/2} = \frac{\langle r^2\rangle^{1/2}}{\sqrt{2A}}, \qquad (18)$$

where $\vec{R}$ is the center-of-mass coordinate. In Fig. 5(a), we plot r_{av} as a function of N, for N increasing from a few hundred to a few thousand bosons. We find that r_{av} increases slowly as expected (as RIB decreases and LIB does not change substantially, and as a consequence, the wave function spreads outward). Finally at $N = 2460$, RIB vanishes and there is no MSR to hold the condensate, we call it a partial collapse. This is also reflected in the sharp fall in r_{av} at $N = 2460$ [Fig. 5(a)]. Thus $N_{cr}^{first} = 2460$. The associated tunneling rate Γ_N^{tunnel} near the first collapse is shown in Fig. 6(a). Near N_{cr}^{first}, the condensate is associated with a large tunneling probability. Thus N_{cr}^{first} is associated with the first branch of the metastable condensate.

With further increase in particle number we observe that the MSR reappears at $N = 2605$, the second branch starts to develop, and the LIB decreases gradually. This is due to the fact that the net attractive interaction now dominates over the effect arising from the anharmonic distortion, as the former increases as $\frac{N(N-1)}{2}$ while the latter increases as N. Due to a substantial increase in attraction, both the height of the LIB and the local minimum of $\omega_0(r)$ decrease rapidly, compared with the decrease of the height of the RIB. Hence the MSR revives. As the LIB decreases, the metastable condensate

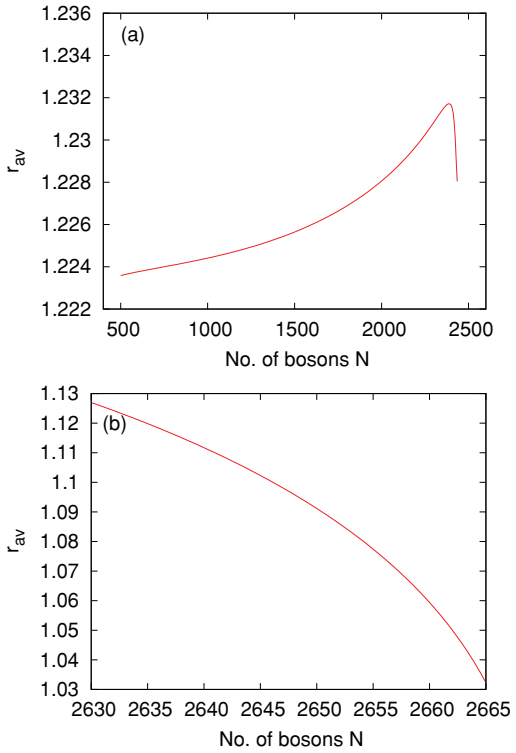

FIG. 5. (Color online) Plot of average size of the attractive condensate r_{av} (in o.u.) as a function of N in the the anharmonic trap ($\lambda = -9.37 \times 10^{-6}$ o.u. and $a_{sc} = -1.832 \times 10^{-4}$ o.u.) near the first [panel (a)] and second [panel (b)] criticality.

shrinks inward, and we observe its behavior to be quite similar to what is seen in a pure harmonic trap: r_{av} decreases sharply with increasing N, as seen in Fig. 5(b). Unlike the first metastable branch, in the second branch the fall of r_{av} is fairly sharp (note the difference in the horizontal scales in the two panels) and quicker collapse occurs at $N = 2667$. We name this as the second criticality (N_{cr}^{second}). We also observe that near the second critical point, the condensate wave function is associated with an oscillatory part in the left side of the LIB. At $N > N_{cr}^{second}$, the entire condensate collapses into the deep well, forming clusters. The associated tunneling rate Γ_N^{tunnel} for the second metastable branch has been calculated using Eqs. (16) and (17) with the limits of the integrations suitably changed and is shown in Fig. 6(b). The physical explanation for the appearance of two distinct metastabilities is as follows. The attractive interaction lowers the effective potential [$\omega_0(r)$] and the amount of lowering increases with N as $\frac{N(N-1)}{2}$. This lowering decreases rapidly

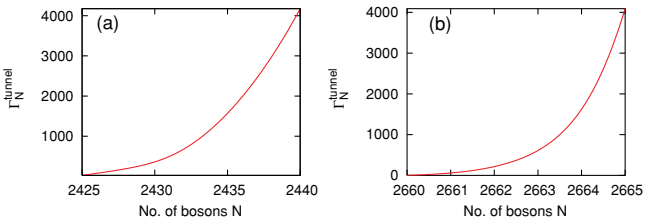

FIG. 6. (Color online) Plot of Γ_N^{tunnel} (in atoms/s) against N near the first (a) and the second (b) criticality.

as r increases. On the other hand, the anharmonic term also lowers the effective potential, but the corresponding lowering is appreciable only for large r and it increases with r as well as with N. The increase with N being roughly proportional to N. Hence, when $|\lambda|$ is not too small and N increases from a small value ($<N_{\rm cr}^{\rm first}$), the lowering due to anharmonicity (first lowering) at large r is much larger than that due to the interaction (second lowering). Hence, with increasing N, $\omega_0(r)$ decreases for large r, giving rise to the first metastability and the appearance of the RIB. As N increases the RIB decreases, leading to the first criticality with the partial collapse at $N = N_{\rm cr}^{\rm first}$. With further increase of N, the second lowering at a smaller r increases faster than the first lowering. This causes reappearance of the MSR, *whose minimum now gradually moves inward*. As N increases even further, the second lowering *for smaller r* increases very rapidly, inducing a deep attractive well and an intermediate barrier on the left (LIB) between this well and the MSR. The second lowering decreases very rapidly with increasing r and is not strong enough at the position of RIB to alter it appreciably. As N increases further, the LIB disappears and the second criticality with collapse at $N = N_{\rm cr}^{\rm second}$ results. However the two branches are discontinuous in the range $2461 \leqslant N \leqslant 2604$ for the present choice of parameter sets. As we have said earlier, there is a competition between the two controllable parameters, viz., interaction and anharmonicity. Thus the existance of the discontinuous metastable branch will strongly depend on the choice of interaction and anharmonic distortion parameters. Our present study considers only a particular value of anharmonic distortion. So further study with other values of λ is essential.

IV. CONCLUSION

In summary, we have applied a correlated many-body method in three dimensions, incorporating a realistic interatomic interaction (van der Waals potential) to study metastable condensates confined in a trapping potential with a finite barrier. The potential is taken as a sum of a quadratic term plus a quartic term, which approximates an optical dipole trap, that is, a harmonic confinement combined with a Gaussian envelope. We obtain the complete quantitative description of the decay process of the quasistationary condensate with both repulsive and attractive interatomic interactions. Due to the use of a realistic interatomic interaction together with interatomic correlations in the many-body wave function and consideration of a finite number of atoms in the trap, our results exhibit a more realistic picture. For a repulsive BEC, the quasi-stationary condensate can be stabilized by controlling the effective two-body interaction (through $a_{\rm sc}$) and also the anharmonicity of the trap. By employing the WKB approximation, we calculate decay rates of such systems, which would be possible to measure experimentally. However, in contrast with earlier findings, in our present calculation no offset potential is required for the transition from a quasibound resonance state to a bound state. This difference is attributed to the use of a realistic interatomic interaction having a hard core at short range which prevents a catastrophic singularity at the origin as in the GP theory and produces a deep but finite well on the left of the LIB. On the other hand, for an attractive BEC, in addition to the usual metastable condensate in a harmonic trap, we observe a new metastable branch which appears only for an intermediate range of particle number below the critical value for collapse due to attractive interaction only. The metastable branch is also associated with an eventual collapse, for which the critical number is $N_{\rm cr}^{\rm first}$. We also determine the decay rates of the metastable BEC due to quantum tunneling from both the metastable regions. However, the transition between these two branches is discontinuous. We have observed that this discontinuity strongly depends on the distortion parameter. However as the decay rate of the ^{85}Rb atom in the new metastable region is quite high, the experimental study of this new phase may be difficult. But this technical difficulty may be circumvented by the proper choice of the parameters.

Prediction of two branches of criticality, in particular, the fact that the criticality associated with the right-side barrier appears and then *disappears* as N increases from a small value up to $N_{\rm cr}^{\rm first}$ and then beyond, are the most significant physics outcome of this work. From a technical point of view, the use of a many-body theory, incorporating *all* two-body correlations in the many-body wave function and a *realistic* finite-range interatomic interaction with a strong short-range repulsion are the realistic features. Deviations from earlier results are attributed to these.

ACKNOWLEDGMENTS

This work has been supported by a grant from the Department of Science and Technology (DST) [Fund No. SR/S2/CMP/0059(2007)], Government of India, under a research project. One of us (SKH) acknowledges the Council of Scientific and Industrial Research. TKD acknowledges the University Grants Commission, India.

[1] D. M. Stamper-Kurn, M. R. Andrews, A. P. Chikkatur, S. Inouye, H. J. Miesner, J. Stenger, and W. Ketterle, Phys. Rev. Lett. **80**, 2027 (1998).
[2] N. Moiseyev, L. D. Carr, B. A. Malomed, and Y. B. Band, J. Phys. B **37**, L193 (2004).
[3] P. Schlagheck and T. Paul, Phy. Rev. A **73**, 023619 (2006).
[4] K. Rapedius, D. Witthaut, and H. J. Korsch, Phys. Rev. A **73**, 033608 (2006).
[5] L. D. Carr, M. J. Holland, and B. A. Malomed, J. Phys. B **38**, 3217 (2005).
[6] S. K. Adhikari, J. Phys. B **38**, 579 (2005).
[7] B. Chakrabarti, T. K. Das, and P. K. Debnath, Phys. Rev. A **79**, 053629 (2009).
[8] T. K. Das and B. Chakrabarti, Phys. Rev. A **70**, 063601 (2004).
[9] T. K. Das, S. Canuto, A. Kundu, and B. Chakrabarti, Phys. Rev. A **75**, 042705 (2007).
[10] T. K. Das, A. Kundu, S. Canuto, and B. Chakrabarti, Phys. Lett. A **373**, 258 (2009).
[11] J. L. Ballot and M. Fabre de la Ripelle, Ann. Phys. (NY) **127**, 62 (1980).

[12] M. Fabre de la Ripelle, Ann. Phys. (NY) **147**, 281 (1983).
[13] C. J. Pethick and H. Smith, *Bose-Einstein Condensation in Dilute Gases* (Cambridge University Press, Cambridge, England, 2002).
[14] C. D. Lin, Phys. Rep. **257**, 1 (1995).
[15] M. Abramowitz and I. A. Stegan, *Handbook of Mathematical Functions* (Dover, New York, 1972), p. 773.
[16] T. K. Das, H. T. Coelho, and M. Fabre de la Ripelle, Phys. Rev. C **26**, 2281 (1982).
[17] M. H. Anderson *et al.*, Science **269**, 198 (1995).
[18] J. L. Roberts, N. R. Claussen, S. L. Cornish, E. A. Donley, E. A. Cornell, and C. E. Wieman, Phys. Rev. Lett. **86**, 4211 (2001); J. L. Roberts, N. R. Claussen, J. P. Burke, C. H. Greene, E. A. Cornell, and C. E. Wieman, *ibid.* **81**, 5109 (1998).
[19] S. L. Cornish, N. R. Claussen, J. L. Roberts, E. A. Cornell, and C. E. Wieman, Phys. Rev. Lett. **85**, 1795 (2000).
[20] S. Stock, V. Bretin, F. Chevy, and J. Dalibard, Europhys. Lett. **65**, 594 (2004).
[21] V. Bretin, S. Stock, Y. Seurin, and J. Dalibard, Phys. Rev. Lett. **92**, 050403 (2004).
[22] G.-Q. Li, L.-B. Fu, J.-K. Xue, X.-Z. Chen, and J. Liu, Phys. Rev. A **74**, 055601 (2006); D. A. Zezyulin, G. L. Alfimov, V. V. Konotop, and V. M. Pérez-García, *ibid.* **78**, 013606 (2008).
[23] J. P. Martikainen, Phys. Rev. A **63**, 043602 (2001).
[24] A. Kundu, B. Chakrabarti, T. K. Das, and S. Canuto, J. Phys. B **40**, 2225 (2007).